Tumor cell-fibroblast heterotypic aggregates in malignant ascites of patients with ovarian cancer

QING HAN[1*], BANGXING HUANG[2*], ZAIJU HUANG[1], JING CAI[1], LANQING GONG[1], YIFAN ZHANG[1], JIAHONG JIANG[1], WEIHONG DONG[1] and ZEHUA WANG[1]

Departments of [1]Obstetrics and Gynecology and [2]Pathology, Union Hospital, Tongji Medical College, Huazhong University of Science and Technology, Wuhan, Hubei 430022, P.R. China

Received June 12, 2019; Accepted September 17, 2019

DOI: 10.3892/ijmm.2019.4361

Abstract. Ascitic multicellular aggregates (MCAs) promote peritoneal metastasis of ovarian cancer. The aim of the present study was to elucidate the role of cancer-associated fibroblasts (CAFs) in MCA formation and metastasis in patients with high-grade serous ovarian cancer (HGSOC). Immunohistochemistry was used to identify the cell phenotypes and the presence of CAFs in ascitic MCAs. The role of CAFs in tumor-cell MCA formation was assessed by co-culture in suspension. Primary ascitic tumor cells and omental CAFs were used to generate *ex vivo* MCAs in hanging drops, and the invasiveness of MCAs was evaluated by mesothelial clearance and adhesion assays *in vitro* and *in vivo*. MCAs containing CAFs and tumor cells were identified in the ascitic fluid. CAFs facilitated tumor cell aggregation and compaction to form MCAs, and enhanced the mesothelial clearance and adhesion abilities of tumor-cell MCAs. These findings suggest that ascitic CAFs promote peritoneal metastasis by forming heterotypic aggregates with tumor cells, and that they may serve as potential targets for the treatment of HGSOC.

Correspondence to: Professor Weihong Dong or Dr Zehua Wang, Department of Obstetrics and Gynecology, Union Hospital, Tongji Medical College, Huazhong University of Science and Technology, 1277 Jiefang Avenue, Wuhan, Hubei 430022, P.R. China
E-mail: rubydwh@126.com
E-mail: zehuawang@163.net

*Contributed equally

Abbreviations: MCAs, multicellular aggregates; CAFs, cancer-associated fibroblasts; HGSOC, high-grade serous ovarian cancer; EOC, epithelial ovarian cancer; α-SMA, α-smooth muscle actin; DMEM/F12, Dulbecco's modified Eagle's medium:nutrient mixture F-12; GFP, green fluorescent protein; IHC, immunohistochemistry; IF, immunofluorescence

Key words: ovarian cancer, cancer-associated fibroblasts, multicellular aggregates, ascites, spheroid, cadherin, heterogeneity

Introduction

Epithelial ovarian cancer (EOC) is the leading cause of gynecological malignancy-associated deaths among women. In 2015, ~52,100 patients were diagnosed with ovarian cancer in China, and ~22,500 succumbed to the disease (1). Due to the incipient protracted nature of the disease and the lack of effective screening and diagnostic methods, the majority of patients (>75%) are diagnosed at an advanced stage when metastasis has already occurred (2). Among patients with advanced disease, the 5-year survival rate is only 29% (3). EOCs predominantly spread through peritoneal dissemination. Malignant ascites is closely associated with poor patient prognosis, and is the most common symptom of disease recurrence. Therefore, insights into the mechanisms that confer a metastatic advantage to tumor cells in the peritoneal cavity may aid in the development of novel therapeutics to improve the prognosis of patients with ovarian cancer.

Given the critical role of ascites in the metastasis and recurrence of ovarian cancer, peritoneal cytological examination is conducted during EOC surgical staging, where the focus is primarily on the presence or absence of malignant cells (4). Indeed, the cellular component of ovarian cancer ascites exhibits a high degree of complexity and heterogeneity. In addition to tumor cells, fibroblasts, mesothelial cells, immature myeloid cells and inflammatory cells have been detected in the malignant ascites of patients with EOC. Ascitic cells can present as single cells or multicellular aggregates (MCAs) (5-8), and MCA formation is considered to be a possible strategy for EOC cell survival in ascites. Cell-cell binding facilitates cell survival by enhancing pro-survival signals in tumor cells, protecting them from anoikis (5). Moreover, there is growing evidence that the MCAs in ovarian cancer ascites are highly malignant and resistant to chemotherapy (9-11). Therefore, MCAs are considered to be the key contributors to secondary lesion formation in peritoneal organs. However, the mechanisms underlying MCA formation in EOC ascites are poorly understood.

Fibroblasts in the tumor microenvironment, also referred to as cancer-associated fibroblasts (CAFs), account for a number of the malignant properties of the tumors, including uncontrolled cell proliferation, reduced apoptosis, angiogenesis, enhanced invasion and migration, and resistance to therapy (12-14).

Previously, an abundance of CAFs, characterized by the expression of α-smooth muscle actin (α-SMA) and fibroblast activation protein, were identified in EOC tissues, and were associated with advanced disease stage and metastasis to the lymph nodes and omentum (15). Moreover, fibroblasts in the omentum were activated in EOC even prior to interaction with tumor cells; omental CAFs contributed to the formation of the pre-metastatic niche, and promoted omental adhesion and implantation of tumor cells (16). These findings suggest that CAFs play a key role in EOC progression. In addition, CAFs can directly bind to EOC cells through the heterotypic adhesion of E-cadherin (E-cad) and N-cadherin (N-cad), which have been found to drive cancer cell invasion (17). However, the direct interaction between CAFs and EOC cells suspended in the peritoneal cavity has yet to be elucidated.

The majority of studies on ascitic MCAs have focused on tumor cells alone, while the other cellular components of ascites have rarely been investigated. In the present study, the presence of tumor cell-CAF heterotypic MCAs ($MCAs^{TC/CAF}$) in EOC ascites and the role of CAFs in MCA formation and peritoneal anchoring were investigated. High-grade serous ovarian carcinoma (HGSOC) is the most common and aggressive subtype of EOC, which usually presents at an advanced stage (stage III or IV) and accounts for 70-80% of ovarian cancer-associated mortality. Therefore, ascitic MCAs obtained from HGSOC patients were assessed in terms of morphology, phenotype and the presence of CAFs. In addition, *in vitro* and *in vivo* experiments were performed using primary ascitic tumor cells obtained from patients with HGSOC; the role of CAFs in MCA formation was subsequently evaluated, and the adhesion and mesothelial clearance properties of $MCAs^{TC/CAF}$ with $MCAs^{TC}$ were compared. The aim of the present study was to provide novel insight into the complex peritoneal microenvironment, hoping to improve the treatment of patients with refractory or recurrent EOC.

Materials and methods

Ascites and omental tissues of patients with HGSOC. Ascitic and omental specimens were obtained from 13 patients with pathologically confirmed HGSOC who underwent surgery at the Union hospital of Tongji Medical College, Huazhong University of Science and Technology (Wuhan, China); 12 of the ascitic specimens were obtained during surgery, and 1 was obtained during abdominal paracentesis for the treatment of malignant ascites. The study protocol was approved by the Ethics Committee of Tongji Medical College, Huazhong University of Science and Technology (IORG0003571) and informed consent was obtained from all participants. The patient clinicopathological characteristics are summarized in Table I.

Immunohistochemical analysis of cell pellets derived from ascites. Within 20 min after ascitic sampling, the ascitic cells were enriched using CytoRich (Red Preservative fluid; 491336; BD Biosciences) according to the manufacturer's instructions, and were subsequently fixed in 4% paraformaldehyde for 1 h and embedded in paraffin. Hematoxylin and eosin (H&E) staining and immunohistochemistry assays were performed; serial sections were deparaffinized and incubated with 3% H_2O_2 for 15 min. Antigen retrieval was conducted using sodium citrate (pH 6.0), and the specimens were blocked with 5% bovine serum albumin (BSA). The sections were then incubated with primary antibodies overnight at 4˚C, and biotinylated-secondary antibodies for 30 min at room temperature. Primary antibodies against E-cad (cat. no. ab76319; 1:500), N-cad (cat. no. ab76011; 1:400), α-SMA (cat. no. ab5694; 1:200), vimentin (cat. no. ab92547; 1:600), fibroblast-specific protein 1 (FSP-1; cat. no. ab197896; 1:250), claudin 4 (cat. no. ab15098; 1:500) and nuclear-associated antigen Ki-67 (cat. no. ab92742, 1:500) were purchased from Abcam. Anti-fibroblast activation protein (FAP; cat. no. AF3715-SP; 1:500) was obtained from R&D, anti-Moc-31 (cat. no. MAB-0280; 1:500) was obtained from Fuzhou Maixin Biotech Co., Ltd., anti-transcription factor paired box 8 (PAX8; cat. no. GR002; 1:200) was purchased from Gene Tech Co., Ltd., anti-calretinin (cat. no. DAK-Calret 1; 1:500) was purchased from Dako (Agilent Technologies, Inc.), and anti-estrogen receptor (ER; pre-diluted) was purchased from Ventana Medical Systems, Inc. The signals were visualized by incubating the sections in freshly prepared 3,3-diaminobenzidin (DAB) solution for 5 min and counterstaining with hematoxylin. PBS substitution for the primary antibody served as the blank control.

Immunofluorescence analysis. Immunofluorescence assays were used to detect the expression of E-cad, N-cad, vimentin and α-SMA in ascitic MCAs. The MCAs were isolated from the ascitic fluid as described by Latifi *et al* (5). Briefly, the cell pellets were seeded on low-adhesive plates in complete medium, and maintained at 37˚C in the presence of 5% CO_2. MCAs were suspended in the medium as spheroids, while adherent cells were attached to the plate surface. After 24 h, spheroids were pipetted and plated onto sterilized coverslips in 24-well plates (cat. no. 702001; Wuxi NEST Biotechnology Co., Ltd.). After a 1-h incubation at 37˚C, the medium was carefully aspirated and the coverslips were washed with PBS. The samples were then fixed in 4% paraformaldehyde for 30 min, followed by permeabilization with ice-cold acetone for 10 min. The cells were then blocked in 10% BSA and incubated with the same primary antibodies as those used for the immunohistochemistry analyses. Secondary Cy3-labeled anti-rabbit IgG (cat. no. 072-01-15-06; KPL, Inc.; 1:1,000) and FITC-labeled anti-rabbit IgG (cat. no. 172-1506, 1:1,000 dilution; KPL, Inc.) were used during the secondary antibody incubation step, and the cells were counterstained with DAPI (1:1,000; Invitrogen; Thermo Fisher Scientific, Inc.).

Primary cell isolation. Cells were isolated from the peritoneal fluid using the Percoll (TBDScience) density gradient centrifugation technique (18). Single-cell suspensions were prepared by trypsinization. The cells were incubated with a PE-labeled mouse anti-human epithelial cell adhesion molecule (EpCAM) antibody (cat. no. ab112068; Abcam) and the EpCAM-positive tumor cells were isolated by fluorescence-activated cell sorting with a MoFlo XDP cell sorter (Beckman Coulter, Inc.). Mesothelial cells were isolated from non-metastatic omentum and CAFs were isolated from metastatic omentum samples of HGSOC patients, as previously described (16). The primary fibroblasts (vimentin-positive and cytokeratin 8-negative) and mesothelial cells (vimentin-positive and cytokeratin 8-posi-

Table I. Clinicopathological characteristics of the HGSOC patients studied.

Patient no	FIGO stage	Age, years	Prior treatment	Peritoneal metastasis						LNM	Experimental methods used
				Fallopian tube	Omentum	Appendix	Parietal peritoneum	Intestinal surface	Liver and diaphragm		
1	IIIC	25	None	Positive	Positive	Positive	Positive	Positive	Negative	Positive	IHC
2	IIA	63	None	Negative	Negative	Negative	Negative	Negative	Negative	Negative	IHC
3	IIIC	49	Cytoreductive surgery followed by TP for 2 cycles	Negative	Positive	Positive	Positive	Positive	Positive	NA	IHC
4	IIIC	65	None	Positive	Positive	NA	Positive	Positive	Positive	Negative	IHC
5	IIIB	45	None	Positive	Positive	NA	Positive	Positive	Negative	Negative	IHC, IF
6	IIIC	66	None	Negative	Positive	Negative	Positive	Positive	Negative	Negative	IHC, IF
7	IIIC	55	None	NA	Positive	NA	Positive	Positive	Negative	NA	IHC
8	IIIC	49	None	Positive	Positive	Positive	Positive	Positive	Negative	Positive	IHC, IF
9	IIIC	67	None	NA	Positive	Positive	Positive	Positive	Negative	NA	IHC, mice
10	IIIC	52	None	Positive	Negative	Negative	Positive	Positive	Negative	Negative	IHC, mice
11	IIIC	54	None	Positive	Positive	NA	Positive	Positive	Positive	NA	IHC
12	IIIC	55	None	Positive	Positive	Negative	Positive	Positive	Positive	NA	IHC
13	IV	58	TP for 6 cycles	Positive	Positive	Positive	Positive	Positive	Negative	NA	Mice

HGSOC, high-grade serous ovarian cancer; FIGO, International Federation of Gynecology and Obstetrics; TP, taxol and platinum chemotherapy; NA, not available; LNM, lymph node metastasis; IHC, immunohistochemistry; IF, immunofluorescence.

tive) were identified using immunocytochemistry. The expression of α-SMA, a marker that distinguishes CAFs from normal fibroblasts, was detected by immunocytochemistry and western blotting. The primary cells were cultured in a humidified 37˚C incubator (5% CO_2) in Dulbecco's modified Eagle's medium:nutrient mixture F-12 (DMEM/F12) containing 10% fetal bovine serum (Gibco; Thermo Fisher Scientific, Inc.) and 1% penicillin-streptomycin. All primary cells used were at passage 2 or 3.

Western blot analysis. Total protein was isolated from CAFs using RIPA buffer (cat. no. P0013C; Beyotime Institute of Biotechnology) and quantified with a bicinchoninic acid protein assay kit as per the manufacturer's protocol (Beyotime Institute of Biotechnology). Each sample (30 μg total protein) was separated by SDS-PAGE on a 12% gel, and transferred to a PVDF membrane (Bio-Rad Laboratories, Inc.) that was pre-treated with methanol. The membrane was blocked, rinsed, and subsequently incubated with primary antibodies against α-SMA (1:500; cat. no. ab5694; Abcam) overnight at 4˚C. After washing, the blots were incubated with the corresponding secondary antibodies, and the labeled proteins were detected using an enhanced chemiluminescence kit (Bio-Rad Laboratories, Inc.). Finally, the signals were visualized using the Bio-Rad Universal Hood II with β-actin as the loading control.

MCA formation assays. The SKOV3 human EOC cell line was purchased from the China Center for Type Culture Collection. A previously generated subline marked with green fluorescent protein (SKOV3-GFP) was also used (19). For MCA formation, tumor cells (SKOV3 or primary ascitic tumor cells) were seeded into 6-well low-adherence plates (cat. no. 3471; Corning Inc.) at $2x10^4$ cells per well, either alone or co-cultured with CAFs (tumor cells:CAFs = 8:1). The cells were cultured in serum-free DMEM/F12 (2 ml per well) containing 2% B27 (cat. no. 12587010; Gibco; Thermo Fisher Scientific, Inc.), 20 ng/ml fibroblast growth factor (cat. no. 100-66-500, PeproTech, Inc.), 20 ng/ml epidermal growth factor (cat. no. AF-100-15-100; PeproTech, Inc.), 10 ng/ml leukemia inhibitory factor (cat. no. 300-05-100; PeproTech, Inc.) and 1% insulin-transferrin-selenium (cat. no. 1933661; Gibco; Thermo Fisher Scientific, Inc.). The MCAs were observed under an inverted microscope (IX73; Olympus Corporation) once daily for 5 days. Images were acquired at a magnification of x100 and five regions were randomly selected for quantitative evaluation of MCA (three-dimensional cell clusters with a diameter of >50 μm) count and size. All assays were performed in triplicate.

MCA hanging drop formation. Tumor cells (SKOV3 and primary ascitic tumor cells from 2 patients) and CAFs were labeled green with PKH67 (Sigma-Aldrich; Merck KGaA) and red with FM4-64 (Thermo Fisher Scientific, Inc.). The tumor cells were suspended in fresh medium at $5x10^3$ cells/ml, with or without CAFs (tumor cells/CAFs = 8:1) to generate $MCAs^{TC/CAF}$ or $MCAs^{TC}$. Droplets (20 μl, 100 tumor cells per droplet) were seeded onto the inner surface of the lid of a tissue culture dish (100 mm diameter; cat. no. 704001; Wuxi NEST Biotechnology Co., Ltd.), and PBS was added to cover the bottom of the dish. The lid was gently inverted atop the dish without mixing the droplets, and cultured at 37˚C for 48 h. The generated MCAs were identified by microscopic examination (IX73; Olympus Corporation). This method was performed as described by Klymenko *et al* (20).

In vitro adhesion assays. Rat tail collagen type I (100 μl, 1.5 mg/ml; BD Biosciences) was placed into 96-well plates (701001, NEST) and incubated at 37˚C for 30 min until gel polymerization. The $MCAs^{TC}$ and $MCAs^{TC/CAF}$ generated by hanging drop formation were seeded onto the collagen layer at a density of 100 MCAs/well and allowed to adhere for 30 min. The total initial fluorescence of each well was determined using a microplate reader (excitation, 490 nm; emission, 520 nm; SpectraMax i3x, Molecular Devices, LLC). Following incubation at 37˚C for 30 min, the MCAs were washed three times with PBS and the fluorescence of the adherent cells was measured again. The adhesion ratio was calculated as $fluorescence^{adhesion}/fluorescence^{initial}$, and all assays were performed in triplicate.

Mesothelial clearance assays. FM4-64-labeled mesothelial cells were cultured in rat tail collagen type I-coated (1.5 mg/ml) 6-well plates to 100% confluence to mimic the mesothelial monolayer covering the peritoneum. $MCAs^{TC}$ and $MCAs^{TC/CAF}$ of SKOV3-GFP cells were applied to the mesothelial cell layer. Following incubation at 37˚C for 7 days, the disaggregation and dispersal of MCAs and the mesothelial clearance area were monitored using a fluorescence microscope (IX73, Olympus Corporation) once daily for 7 days. The mesothelial clearance area was quantified using ImageJ software, version 1.48 (National Institutes of Health). The assays were performed in triplicate.

In vivo adhesion assays. The following animal experiments were approved by the Institutional Animal Care and Use Committee at Tongji Medical College. Female BALB/c nude mice were purchased from Beijing HFK Bioscience Co., Ltd., and housed in a standard pathogen-free environment. To detect the adhesion ability of MCAs *in vivo*, the $MCAs^{TC}$ and $MCAs^{TC/CAF}$ generated in hanging drops were injected into the peritoneal cavities of the mice (n=3/group, 500 MCAs per mouse). The animals were anesthetized using 2.5% isoflurane for 5 min and then euthanized by cervical dislocation 4 h after injection, and the mesentery, parietal peritoneum and omentum were removed. After washing the tissues with PBS to remove unattached tumor cells, the tissues were observed under a fluorescence microscope and the fluorescence intensity was analyzed using ImageJ software, version 1.48.

Statistical analysis. All numerical data are presented as mean ± standard deviation. The differences between the $MCAs^{TC}$ and $MCAs^{TC/CAF}$ groups were analyzed by Student's t-test using GraphPad Prism 5 (GraphPad Software, Inc.), and $P<0.05$ was considered to indicate a statistically significant difference.

Results

Heterogeneous MCAs in malignant ascites. MCAs, were defined as three-dimensional cell clusters (spheroids) with a

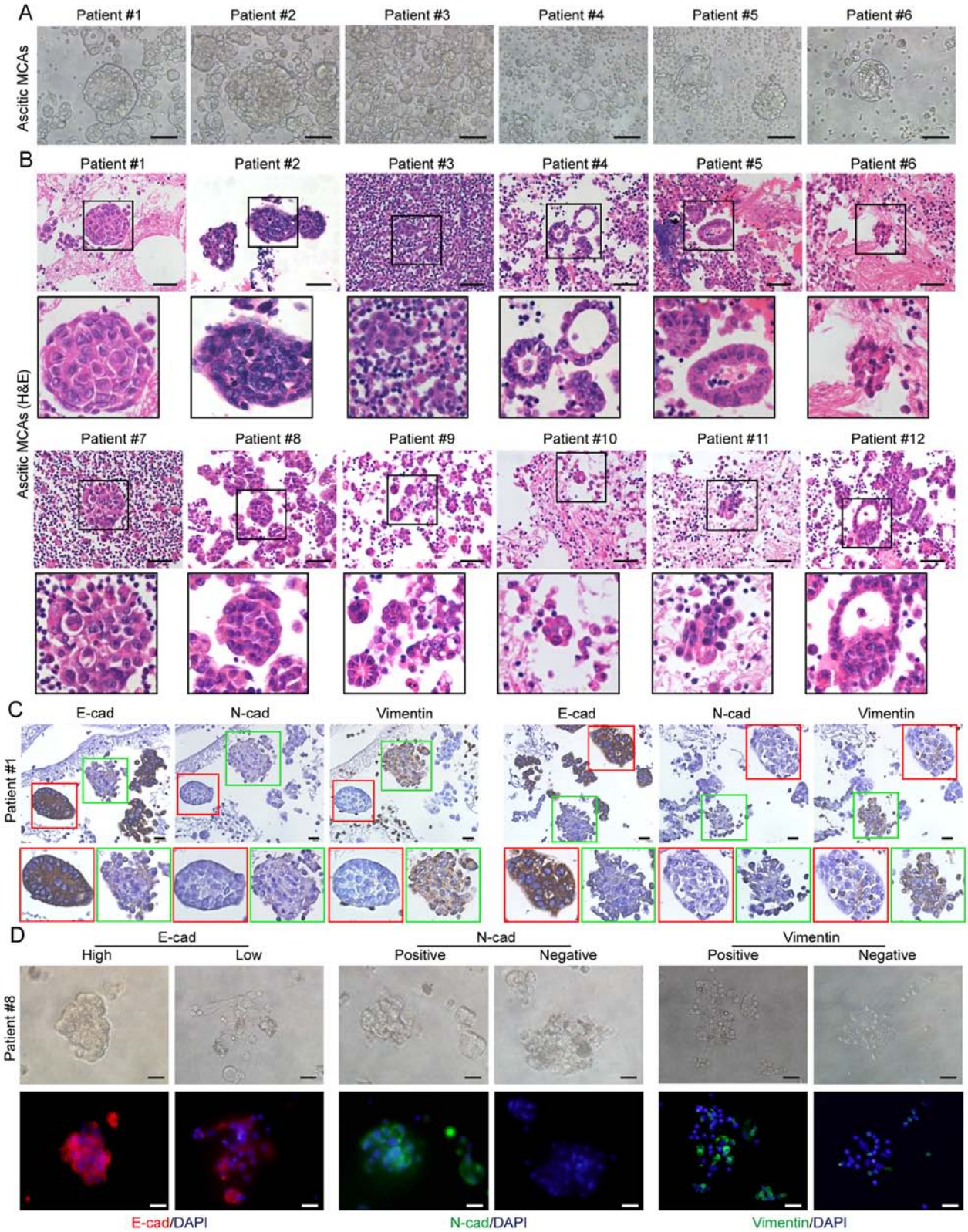

Figure 1. MCA morphology in ascites. (A) Phase-contrast image and (B) hematoxylin and eosin staining of primary MCAs in ascites obtained from patients with high-grade serous ovarian cancer. Scale bars, 50 μm. (C) Representative images of immunohistochemical detection of E-cadherin, N-cadherin and vimentin expression in individual ascitic MCAs. Scale bars, 50 μm. (D) Representative images of immunofluorescence assays for E-cadherin (red), N-cadherin (green) and vimentin (green) expression in ascitic MCAs. Cell nuclei were labeled with DAPI (blue). In individual patients, the MCAs have mixed expression patterns of E-cadherin, N-cadherin and vimentin. Scale bar, 20 μm. MCA, multicellular aggregate.

diameter >50 μm at the widest point. MCAs were detected in all ascitic patient samples, varying in shape and size between patients, as well as between MCAs within individual patients (Fig. 1A). H&E staining revealed the more complex structure of MCAs that presented as spheroids or irregularly shaped cell clusters, with varying sizes and levels of compaction (Fig. 1B).

Notably, some spherical aggregates displayed a monolayer of polarized cells at their surface, and a core of disorganized cells (Fig. 1B).

Next, the expression of the epithelial marker E-cad and the mesothelial markers N-cad and vimentin was analyzed in ascitic cells using immunohistochemistry; two expression patterns were identified in the MCAs: The majority of the MCAs exhibited high levels of E-cad expression, and were N-cad- and vimentin-negative, while few MCAs expressed N-cad and vimentin with low levels of E-cad. The E-cad^{high}/N-cad^{negative} MCAs were more compact compared with those composed of E-cad^{low}/N-cad^{positive} cells (Fig. 1C). Moreover, the phenotypic heterogeneity of ascitic MCAs was confirmed by E-cad, N-cad and vimentin detection (Fig. 1D).

Presence of tumor cell-fibroblast heterotopic MCAs in malignant ascites. To identify the MCAs harboring CAFs, ascitic cell sediments were analyzed using immunohistochemistry for the CAF-specific marker α-SMA. Although most MCAs were α-SMA-negative, MCAs containing α-SMA-positive cells (MCAs$^{TC/CAF}$) were detected in all patients with HGSOC (Fig. 2A). However, the MCAs$^{TC/CAF}$ did not differ morphologically from the MCAs without CAFs, as they both varied in size, shape and compaction level. In these solid spherical aggregates, the unorganized central cells were primarily α-SMA-positive (Fig. 2A). The presence of CAFs in the ascitic MCAs was further confirmed by immunofluorescence detection of α-SMA (Fig. 2B), and by the positive expression of FSP-1 and FAP (Fig. S1). Moreover, the majority of the cells within the MCAs were positive for Moc-31 (epithelial tumor marker), PAX8 (ovarian cancer marker) and Ki-67 expression, and negative for expression of mesothelial markers, including claudin 4, calretinin and ER (Fig. S2), suggesting that MCAs were predominantly composed of tumor cells.

CAFs promote MCA formation. To elucidate the role of CAFs in MCA formation in malignant ascites, MCA formation assays were performed with tumor cells alone or with tumor cells and CAFs. In addition to SKOV3 cells, primary tumor cells obtained from the ascitic fluid of HGSOC patients were used (Fig. 3A). The primary CAFs isolated from the metastatic omentum of HGSOC patients were identified by their typical spindled shape, parallel arrangement, positive expression of vimentin and α-SMA, and the absence of cytokeratin 8 expression (Fig. 3B). Western blot analysis was used to confirm α-SMA expression in the CAFs of the first three generations (Fig. 3C). After culture in suspension for 5 days, the MCAs in the tumor cell-CAF group (with 1/8 of CAFs) were significantly larger and more numerous compared with the tumor cell MCAs (Fig. 3D-F). Moreover, CAFs and SKOV3 cells were combined at ratios of 1:8, 1:5 and 1:1 with a fixed number of SKOV3 cells, and cultured for 5 days. The number and size of the MCAs was found to increase with an increasing proportion of CAFs from 0 to 1:8 and 1:5 (Fig. S3). These findings highlight the role of CAFs in MCA formation.

To observe the interaction between CAFs and tumor cells during MCA formation, CAFs pre-stained with FM464 and SKOV3-GFP were cultured in suspension. The CAFs were linked by filopodia and assembled in a dynamic scaffolding that rescued the tumor cells. At 4 h post-seeding, a number of tumor cells were attached to the CAFs, forming small MCAs that aggregated into larger MCAs through the CAF scaffolding. At 3 days post-seeding, MCA compaction was observable (Fig. 3G). These findings suggest that CAFs promote the aggregation and compaction of tumor cells through intercellular adhesion and pulling.

MCAsTC/CAF are more invasive compared with MCAsTC. To investigate the role of MCAs$^{TC/CAF}$ in the peritoneal metastasis of EOC, *ex vivo* MCAs$^{TC/CAF}$ were generated in hanging drops using primary fibroblast and SKOV3 cells, or primary tumor cells that had been stained with FM4-64 and PKH67, respectively. MCAs containing only tumor cells (MCAs^{TC}) served as the control (Fig. 4A). The presence of CAFs in the MCAs$^{TC/CAF}$ was confirmed by fluorescence analysis (Fig. 4B).

The peritoneum is lined by a mesothelial monolayer, and tumor cell adhesion to the mesothelial cells (and subsequent mesothelial clearance) has been proposed as the first step in peritoneal lesion formation (21-23). To compare the mesothelial-cell clearance capacity of MCAs$^{TC/CAF}$ and MCAs^{TC}, primary mesothelial cells were isolated from human omentum tissues, which were characterized by a cobblestone appearance and positive expression of cytokeratin 8 and vimentin (Fig. 4C). The MCAs generated in hanging drops were seeded on completely confluent mesothelial cells and the area of mesothelial clearance was evaluated (Fig. 4D). The tumor cells in the MCAs$^{TC/CAF}$ group proliferated more rapidly and facilitated a significantly enhanced mesothelial clearance compared with the MCAs^{TC} group (Fig. 4E and F).

To determine whether CAFs promote tumor-cell anchorage to the sub-mesothelial connective tissue matrix, *in vitro* adhesion assays were performed, revealing that the MCAs$^{TC/CAF}$ exhibited enhanced adhesion to collagen (Fig. 4G). Moreover, *in vivo* adhesion assays (Fig. 4H) revealed that significantly more tumor cells attached to the mesentery, parietal peritoneum and omentum in the MCAs$^{TC/CAF}$ group compared with the MCAs^{TC} group (Fig. 4I and J).

Discussion

The majority of solid tumors disseminate via the hematological or lymphovascular system, of which the underlying mechanisms have been widely investigated; however, peritoneal dissemination occurs primarily in patients with ovarian cancer and gastrointestinal neoplasms, and the factors regulating peritoneal metastasis remain to be fully elucidated. To the best of our knowledge, the present study is the first to provide clinical evidence of the presence of ascitic MCAs$^{TC/CAF}$ in patients with HGSOC. CAFs were found to serve as a scaffolding to aggregate free-floating ovarian cancer cells, forming heterotypic MCAs with enhanced peritoneal adhesion and invasion properties. These findings highlight the role of ascitic CAFs in the peritoneal dissemination of HGSOC.

Furthermore, MCAs were found to be present in the peritoneal fluid of all recruited HGSOC patients. Thus, it was proposed that cell-cell adhesion molecules, particularly E-cad and N-cad, are required for spheroid formation in ascites (24,25). The cells in the MCAs were predominantly E-cad-positive, and had a polarized epithelial phenotype. Moreover, the MCAs of E-cad^{high}/N-cad^{negative} cells were more

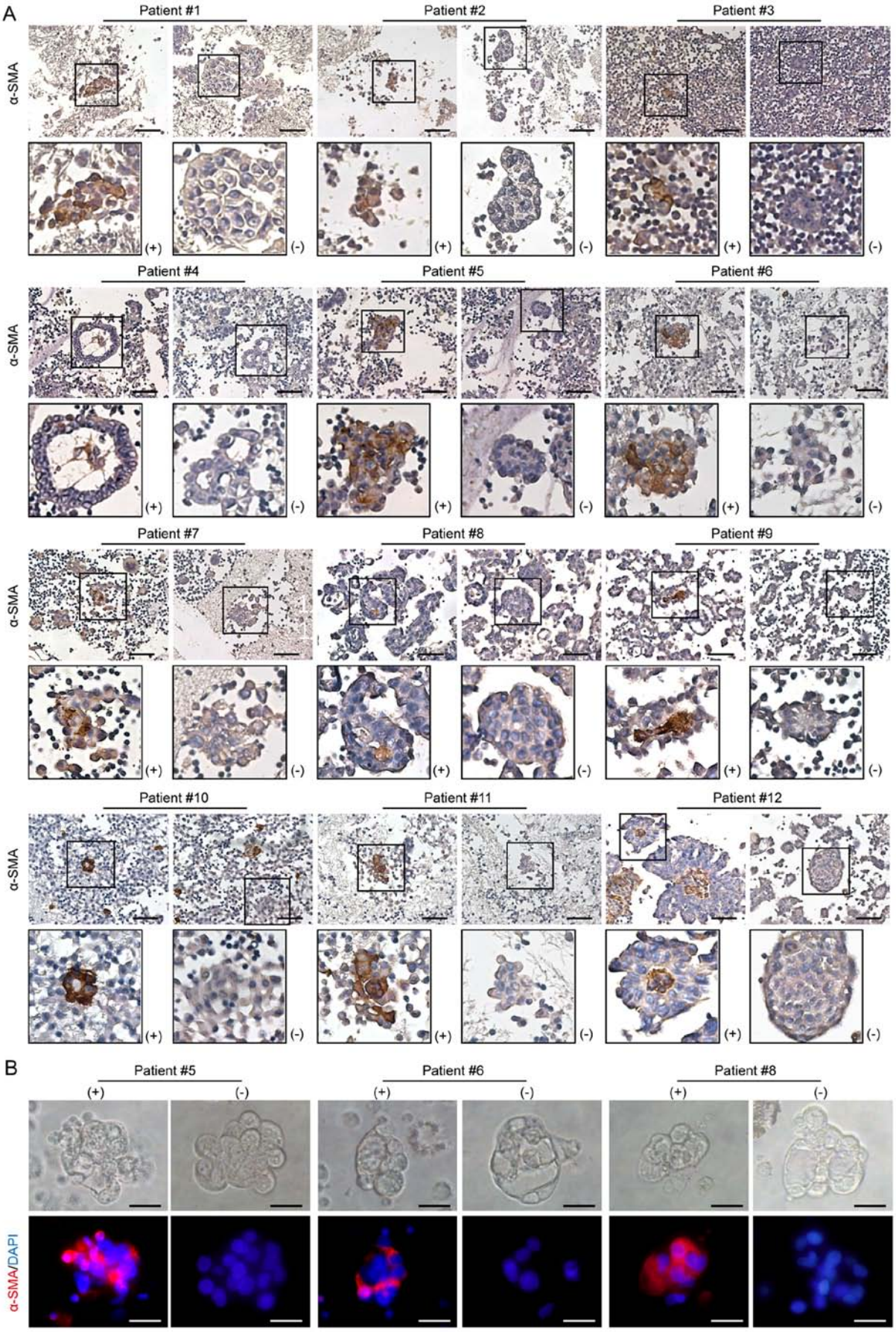

Figure 2. Presence of CAFs in ascitic MCAs. (A) Representative images of immunohistochemistry staining for α-SMA expression in ascitic MCAs. α-SMA-positive MCAs were found in all 12 patients studied. Scale bars, 50 μm. (B) Representative images of immunofluorescence assays for α-SMA (red) in MCAs. Cell nuclei were labeled with DAPI (blue). In individual patients, both α-SMA-positive and α-SMA-negative MCAs were observed. Scale bar, 20 μm. CAFs, cancer-associated fibroblasts; MCAs, multicellular aggregates; α-SMA, α-smooth muscle actin.

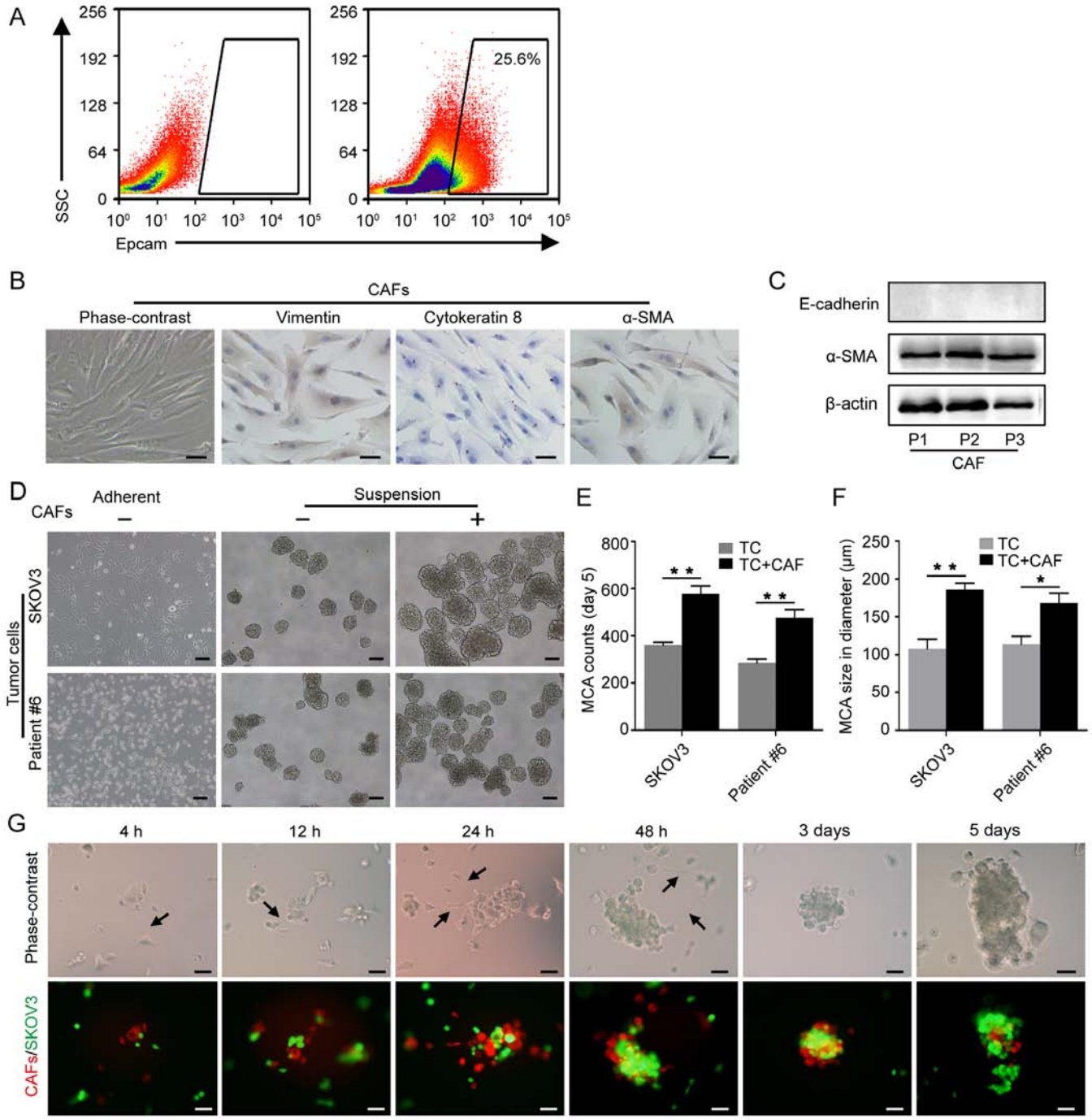

Figure 3. CAFs promote MCA formation. (A) EpCAM^{+} tumor cells were isolated from the ascitic fluid by flow cytometric cell sorting. (B) Identification of primary CAFs isolated from omentum with metastasis; spindle-shaped, vimentin-positive, cytokeratin 8-negative and α-SMA-positive characterization. Scale bars, 50 μm. (C) Western blot analysis of α-SMA expression in primary CAFs; passage 1-3. (D) Representative images of MCA formation assays. SKOV3 and primary tumor cells isolated from patient #6 were cultured alone or co-cultured with CAFs in suspension. Scale bars, 100 μm. (E) Histograms show the MCA counts from the MCA formation assays. (F) Histograms show MCA size in the MCA formation assays. *P<0.05 and **P<0.01. (G) The dynamic process of tumor cell-CAF MCA formation. CAFs and SKOV3 cells were labeled with FM4-64 (red) and GFP (green), respectively. Black arrows indicate the filopodia of CAFs. Scale bars, 50 μm. CAFs, cancer-associated fibroblasts; MCA, multicellular aggregate; α-SMA, α-smooth muscle actin.

compact compared with those of E-cad^{low}/N-cad^{positive} cells. In the initial phases of hematogenous metastasis of solid tumors, tumor cells usually undergo epithelial-to-mesenchymal transition (EMT), during which epithelial cells lose their polarity and cell-cell adhesive properties to acquire the migratory and invasive mesenchymal phenotype accompanied by decreased expression of E-cad, and increased expression of N-cad and vimentin (26). However, due to the unique transcoelomic route of ovarian cancer, by which tumor cells are released directly into the peritoneal cavity, EMT is not considered a prerequisite for EOC metastasis (8,26). Thus, the high E-cad expression in ascitic tumor cells was not unexpected. Moreover, a small number of E-cad^{high}/N-cad^{negative} MCAs were identified. Previous studies have demonstrated that ~30% of human ovarian tumors exhibit simultaneous positive immunoreactivity for both E-cad and N-cad (20,26). Homophilic

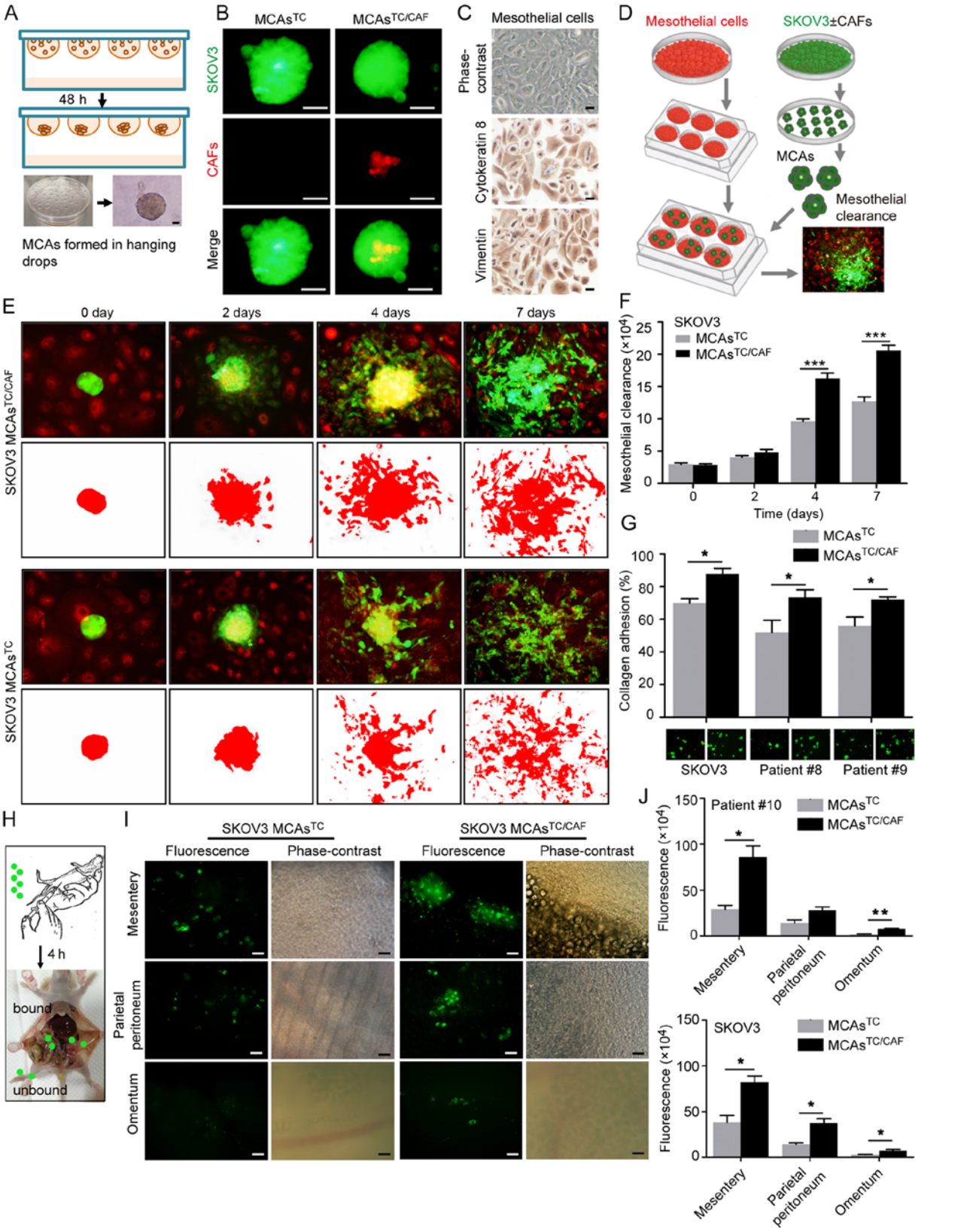

Figure 4. MCAs$^{TC/CAF}$ have a higher invasive capacity than MCAs^{TC}. (A) Schematic diagram of MCA formation in hanging drops. (B) MCAs$^{TC/CAF}$ and MCAs^{TC} morphology by fluorescence microscope. CAFs and SKOV3 cells were labeled with FM4-64 (red) and GFP (green), respectively. Scale bar, 50 μm. (C) Identification of primary mesothelial cells. Mesothelial cells are cytokeratin 8- and vimentin-positive. Scale bars, 50 μm. (D) Schematic diagram of mesothelial clearance assays. (E) Representative images of mesothelial clearance assays with SKOV3 MCAs$^{TC/CAF}$ and MCAs^{TC} at 0, 2, 4 and 7 days. Mesothelial cells and SKOV3 cells were labeled with FM4-64 (red) and GFP (green), respectively. (F) Histograms show that SKOV3 MCAs$^{TC/CAF}$ have a stronger mesothelial clearance ability than SKOV3 MCAs^{TC}. (G) *In vitro* adhesion assays. Histograms show that MCAs$^{TC/CAF}$ have a stronger collagen adhesion capacity than MCAs^{TC}. (H) Schematic diagram of adhesion assays *in vivo*. MCAs were intraperitoneally injected into mice (N=3/group). After 4 h, the mice were sacrificed and the tumor cells bound to the peritoneum were evaluated under a microscope. (I) Representative images of adhesion assays *in vivo*. Tumor cell attachment to the mesentery, parietal peritoneum and omentum. (J) Histograms show the differences in tumor cell florescence intensity in the mesentery, parietal peritoneum, and omentum between groups. *P<0.05, **P<0.01 and ***P<0.001. MCA, multicellular aggregate; CAFs, cancer-associated fibroblasts; TC, tumor cell; GFP, green fluorescent protein.

E-cad/E-cad bonds have been found to be stronger compared with homophilic N-cad bonds (27), which partly explains the different compaction levels observed between MCAs with different cadherin expression patterns in the present study. However, a recent study reported that N-cad-positive ovarian cancer cells formed stable, highly cohesive solid spheroids, whereas E-cad-positive cells generated loosely adhesive cell clusters *in vitro* (28), which is not in line with the observations of the present study. This discrepancy suggests that, besides cadherin expression in tumor cells, additional mechanisms may be involved in ascitic MCA formation.

Non-cancerous cells within the ascitic fluid of patients with ovarian cancer include inflammatory cells, fibroblasts, immature myeloid cells and mesothelial cells (29). The involvement of these cells in ascitic tumor-cell MCAs has not been extensively investigated. Burleson *et al* (30) observed mesothelial and inflammatory cell incorporation, along with tumor cells, into MCAs in malignant ascites; mesothelial cells can facilitate cancer stem-like properties in spheroids of ovarian cancer cells, and promote their peritoneal dissemination (31). In the present study, MCAs harboring CAFs and tumor cells were detected in the ascites of patients with HGSOC, and CAFs were able to recruit tumor cells and promote MCA formation. However, CAFs were only present in a small fraction of the ascitic MCAs, which may be due to the limited number of CAFs, as they predominantly appeared in MCAs, while single CAFs were rare. Labernadie *et al* (17) demonstrated that the heterotypic adhesion of CAFs and cancer cells may be mediated by N-cad at the CAF membrane and E-cad at the cancer cell membrane. Indeed, heterophilic N-cad/E-cad junctions have been demonstrated to exhibit higher binding affinity compared with homophilic E-cad/E-cad junctions (32), which may be the molecular basis of tumor cell-CAF heterotypic adhesion.

CAFs have been proposed to display cancer cell properties in multiple ways, including the secretion of growth factors and chemokines, contact-mediated signaling and direct mechanical interactions (17,33,34). The present study revealed that tumor cell MCAs containing CAFs exhibited enhanced mesothelial clearance and peritoneal adhesion abilities compared with those without CAFs, indicating the supportive role of CAFs in HGSOC peritoneal dissemination mediated by MCAs; however, the underlying mechanisms remain elusive. Davidowitz *et al* (35) discovered that tumor cells expressing mesenchymal markers exhibited enhanced mesothelial clearance ability. The interaction between tumor cells and the sub-mesothelial matrix also depends on the expression of cell surface adhesion molecules, such as integrins (36). Thus, to elucidate the mechanisms by which CAFs promote MCA peritoneal metastasis, further investigations should focus on the effects of incorporated CAFs on the expression of adhesion molecules in tumor cells.

The results of the present study suggest that CAFs in the ascitic fluid of HGSOC patients facilitate tumor cell aggregation and enhance the mesothelial clearance and peritoneal adhesion abilities of tumor cells in MCAs. These findings may provide new insight into the complex peritoneal microenvironment, where CAFs contribute to carcinomatosis by forming heterotypic aggregates with tumor cells. This suggests that the cell-cell interactions between tumor cells and CAFs may be a potential target for the treatment of ovarian cancer (20).

Acknowledgements

Not applicable.

Funding

The present study was supported by the National Natural Science Foundation of China (grant nos. 81472443 and 81572572).

Availability of data and materials

All the datasets generated and analyzed during the present study are available from the corresponding author on reasonable request.

Authors' contributions

ZW and WD designed the present study. ZW and JC supervised the project. QH tended to the technical details and performed the functional experiments. BH performed immunohistochemistry. LG and JJ performed the animal experiments. ZH provided technical support. LG and JJ analyzed and interpreted the data. YZ collected the data and drafted the manuscript in consultation with BH and QH. JC revised the manuscript substantively. All authors contributed to producing the manuscript and have approved the final version of the manuscript for publication.

Ethics approval and consent to participate

The study protocol was approved by the Ethics Committee of Tongji Medical College, Huazhong University of Science and Technology (IORG0003571) and informed consent was obtained from all participants.

Patient consent for publication

Not applicable.

Competing interests

All the authors declare that they have no competing interests.

References

1. Chen W, Zheng R, Baade PD, Zhang S, Zeng H, Bray F, Jemal A, Yu XQ and He J: Cancer statistics in China, 2015. CA Cancer J Clin 66: 115-132, 2016.
2. Vaughan S, Coward JI, Bast RC Jr, Berchuck A, Berek JS, Brenton JD, Coukos G, Crum CC, Drapkin R, Etemadmoghadam D, *et al*: Rethinking ovarian cancer: Recommendations for improving outcomes. Nat Rev Cancer 11: 719-725, 2011.
3. Siegel RL, Miller KD and Jemal A: Cancer Statistics, 2017. CA Cancer J Clin 67: 7-30, 2017.
4. Morgan RJ Jr, Armstrong DK, Alvarez RD, Bakkum-Gamez JN, Behbakht K, Chen LM, Copeland L, Crispens MA, DeRosa M, Dorigo O, *et al*: Ovarian cancer, version 1.2016, NCCN clinical practice guidelines in oncology. J Natl Compr Cancer Netw 14: 1134-1163, 2016.
5. Latifi A, Luwor RB, Bilandzic M, Nazaretian S, Stenvers K, Pyman J, Zhu H, Thompson EW, Quinn MA, Findlay JK and Ahmed N: Isolation and characterization of tumor cells from the ascites of ovarian cancer patients: Molecular phenotype of chemoresistant ovarian tumors. PLoS One 7: e46858, 2012.

6. Davidson B: Ovarian carcinoma and serous effusions. Changing views regarding tumor progression and review of current literature. Anal Cell Pathol 23: 107-128, 2001.
7. Kenny HA, Dogan S, Zillhardt M, Mitra KA, Yamada SD, Krausz T and Lengyel E: Organotypic models of metastasis: A three-dimensional culture mimicking the human peritoneum and omentum for the study of the early steps of ovarian cancer metastasis. Cancer Treat Res 149: 335-351, 2009.
8. Shield K, Ackland ML, Ahmed N and Rice GE: Multicellular spheroids in ovarian cancer metastases: Biology and pathology. Gynecol Oncol 113: 143-148, 2009.
9. Iwanicki MP, Davidowitz RA, Ng MR, Besser A, Muranen T, Merritt M, Danuser G, Ince TA and Brugge JS: Ovarian cancer spheroids use myosin-generated force to clear the mesothelium. Cancer Discov 1: 144-157, 2011.
10. Brodsky AS, Fischer A, Miller DH, Vang S, MacLaughlan S, Wu HT, Yu J, Steinhoff M, Collins C, Smith PJ, *et al*: Expression profiling of primary and metastatic ovarian tumors reveals differences indicative of aggressive disease. PLoS One 9: e94476, 2014.
11. Ip CK, Yung S, Chan TM, Tsao SW and Wong AS: p70 S6 kinase drives ovarian cancer metastasis through multicellular spheroid-peritoneum interaction and P-cadherin/b1 integrin signaling activation. Oncotarget 5: 9133-9149, 2014.
12. Dasari S, Fang Y and Mitra AK: Cancer associated fibroblasts: Naughty neighbors that drive ovarian cancer progression. Cancers (Basel) 10: pii: E406, 2018.
13. Barbazan J and Matic Vignjevic D: Cancer associated fibroblasts: Is the force the path to the dark side? Curr Opin Cell Biol 56: 71-79, 2018.
14. Ireland LV and Mielgo A: Macrophages and fibroblasts, key players in cancer chemoresistance. Front Cell Dev Biol 6: 131, 2018.
15. Zhang Y, Tang H, Cai J, Zhang T, Guo J, Feng D and Wang Z: Ovarian cancer-associated fibroblasts contribute to epithelial ovarian carcinoma metastasis by promoting angiogenesis, lymphangiogenesis and tumor cell invasion. Cancer Lett 303: 47-55, 2011.
16. Cai J, Tang H, Xu L, Wang X, Yang C, Ruan S, Guo J, Hu S and Wang Z: Fibroblasts in omentum activated by tumor cells promote ovarian cancer growth, adhesion and invasiveness. Carcinogenesis 33: 20-29, 2012.
17. Labernadie A, Kato T, Brugues A, Serra-Picamal X, Derzsi S, Arwert E, Weston A, González-Tarragó V, Elosegui-Artola A, Albertazzi L, *et al*: A mechanically active heterotypic E-cadherin/N-cadherin adhesion enables fibroblasts to drive cancer cell invasion. Nat Cell Biol 19: 224-237, 2017.
18. Timonen T, Ortaldo JR and Herberman RB: Characteristics of human large granular lymphocytes and relationship to natural killer and K cells. J Exp Med 153: 569-582, 1981.
19. Guo J, Cai J, Zhang Y, Zhu Y, Yang P and Wang Z: Establishment of two ovarian cancer orthotopic xenograft mouse models for in vivo imaging: A comparative study. Int J Oncol 51: 1199-1208, 2017.
20. Klymenko Y, Johnson J, Bos B, Lombard R, Campbell L, Loughran E and Stack MS: Heterogeneous cadherin expression and multicellular aggregate dynamics in ovarian cancer dissemination. Neoplasia 19: 549-563, 2017.
21. Wintzell M, Hjerpe E, Avall Lundqvist E and Shoshan M: Protein markers of cancer-associated fibroblasts and tumor-initiating cells reveal subpopulations in freshly isolated ovarian cancer ascites. BMC Cancer 12: 359, 2012.
22. Kenny HA, Nieman KM, Mitra AK and Lengyel E: The first line of intra-abdominal metastatic attack: Breaching the mesothelial cell layer. Cancer Discov 1: 100-102, 2011.
23. Kenny HA, Krausz T, Yamada SD and Lengyel E: Use of a novel 3D culture model to elucidate the role of mesothelial cells, fibroblasts and extra-cellular matrices on adhesion and invasion of ovarian cancer cells to the omentum. Int J Cancer 121: 1463-1472, 2007.
24. Yoshida-Noro C, Suzuki N and Takeichi M: Molecular nature of the calcium-dependent cell-cell adhesion system in mouse teratocarcinoma and embryonic cells studied with a monoclonal antibody. Dev Biol 101: 19-27, 1984.
25. Takeichi M: The cadherins: Cell-cell adhesion molecules controlling animal morphogenesis. Development 102: 639-655, 1988.
26. Hudson LG, Zeineldin R and Stack MS: Phenotypic plasticity of neoplastic ovarian epithelium: Unique cadherin profiles in tumor progression. Clin Exp Metastasis 25: 643-655, 2008.
27. Chu YS, Thomas WA, Eder O, Pincet F, Perez E, Thiery JP and Dufour S: Force measurements in E-cadherin-mediated cell doublets reveal rapid adhesion strengthened by actin cytoskeleton remodeling through Rac and Cdc42. J Cell Biol 167: 1183-1194, 2004.
28. Klymenko Y, Kim O and Stack MS: Complex determinants of epithelial: Mesenchymal phenotypic plasticity in ovarian cancer. Cancers (Basel) 9: pii: E104, 2017.
29. Kim S, Kim B and Song YS: Ascites modulates cancer cell behavior, contributing to tumor heterogeneity in ovarian cancer. Cancer Sci 107: 1173-1178, 2016.
30. Burleson KM, Casey RC, Skubitz KM, Pambuccian SE, Oegema TR Jr. and Skubitz AP: Ovarian carcinoma ascites spheroids adhere to extracellular matrix components and mesothelial cell monolayers. Gynecol Oncol 93: 170-181, 2004.
31. Shishido A, Mori S, Yokoyama Y, Hamada Y, Minami K, Qian Y, Wang J, Hirose H, Wu X, Kawaguchi N, *et al*: Mesothelial cells facilitate cancer stemlike properties in spheroids of ovarian cancer cells. Oncol Rep 40: 2105-2114, 2018.
32. Vendome J, Felsovalyi K, Song H, Yang Z, Jin X, Brasch J, Harrison OJ, Ahlsen G, Bahna F, Kaczynska A, *et al*: Structural and energetic determinants of adhesive binding specificity in type I cadherins. Proc Natl Acad Sci USA 111: E4175-E4184, 2014.
33. Astin JW, Batson J, Kadir S, Charlet J, Persad RA, Gillatt D, Oxley JD and Nobes CD: Competition amongst Eph receptors regulates contact inhibition of locomotion and invasiveness in prostate cancer cells. Nat Cell Biol 12: 1194-1204, 2010.
34. Takai Y, Miyoshi J, Ikeda W and Ogita H: Nectins and nectin-like molecules: Roles in contact inhibition of cell movement and proliferation. Nat Rev Mol Cell Biol 9: 603-615, 2008.
35. Davidowitz RA, Iwanicki MP and Brugge JS: In vitro mesothelial clearance assay that models the early steps of ovarian cancer metastasis. J Vis Exp: pii: 3888, 2012.
36. Schlaeppi M, Ruegg C, Tran-Thang C, Chapuis G, Tevaearai H, Lahm H and Sordat B: Role of integrins and evidence for two distinct mechanisms mediating human colorectal carcinoma cell interaction with peritoneal mesothelial cells and extracellular matrix. Cell Adhes Commun 4: 439-455, 1997.